~~CONFIDENTIAL~~

NACA

NASA ltr dtd Nov. 27, 1962. By HLR

RESEARCH MEMORANDUM

Nov. 14, 1962, s/ Boyd C. Myers II.
Effective date: April 23, 1962.

for the

U. S. Air Force

EFFECT OF SEVERAL JET-ENGINE AIR-INLET

CONFIGURATIONS ON THE LOW-SPEED STATIC LONGITUDINAL

STABILITY CHARACTERISTICS AND QUANTITY FLOW OF A

1/6-SCALE MODEL OF THE MX-1764 AIRPLANE

By Delwin R. Croom

Langley Aeronautical Laboratory
Langley Field, Va.

NATIONAL ADVISORY COMMITTEE
FOR AERONAUTICS
WASHINGTON

~~CONFIDENTIAL~~

NATIONAL ADVISORY COMMITTEE FOR AERONAUTICS

RESEARCH MEMORANDUM

for the

U. S. Air Force

EFFECT OF SEVERAL JET-ENGINE AIR-INLET

CONFIGURATIONS ON THE LOW-SPEED STATIC LONGITUDINAL

STABILITY CHARACTERISTICS AND QUANTITY FLOW OF A

1/6-SCALE MODEL OF THE MX-1764 AIRPLANE

By Delwin R. Croom

SUMMARY

An investigation was made in the Langley 300 MPH 7- by 10-foot tunnel
to determine the effect of wing-root leading-edge and scoop-type jet-engine
air-inlet configurations on the static longitudinal stability character-
istics and the duct-flow characteristics of a 1/6-scale model of the
MX-1764 airplane.

The addition of the inlet configurations to the model generally
resulted in slight reductions in longitudinal stability and increases of
maximum lift coefficient. Pressure data at a survey station located near
the duct exit for the model with all intake configurations are presented
without analysis.

INTRODUCTION

An investigation was made in the Langley 300 MPH 7- by 10-foot tunnel
of a 1/6-scale model of the MX-1764 airplane. The objective of the inves-
tigation was to make a preliminary evaluation of the effect of several
jet-engine air-inlet configurations on the static longitudinal stability
characteristics and duct air-flow characteristics of the model. A limited
investigation was also made of the longitudinal control. The duct-flow
characteristics were determined at one survey station located near the
exit of the duct. The angle-of-attack range for this investigation was
from approximately -6° to the stall.

▬▬▬▬▬▬

SYMBOLS

The results of the tests are presented as standard NACA coefficients of forces and moments about the stability axes. (See fig. 1.) The positive direction of forces, moments, and angles is also shown in figure 1. The moment coefficients are given about the 25-percent-wing-mean-aerodynamic-chord position (center of gravity) as shown in figure 2. The coefficients and symbols are defined as follows:

C_L lift coefficient, $\text{Lift}/q_o S$

C_X longitudinal-force coefficient, $X/q_o S$

C_m pitching-moment coefficient, $M/q_o S\bar{c}$

$\left.\begin{array}{c} \dfrac{H_o - H_1}{H_o - p_o} \\[2ex] \dfrac{H_o - p_1}{H_o - p_o} \end{array}\right\}$ pressure coefficients

X force along X-axis, lb

Z force along Z-axis, lb; lift equals $-Z$

M pitching moment, ft-lb

q_o free-stream dynamic pressure, $\rho V_o^2/2$, lb/sq ft

S wing area, sq ft

$\bar{c}$ wing mean aerodynamic chord, ft

V_o free-stream velocity, ft/sec

ρ mass density of air, slugs/cu ft

α angle of attack of fuselage reference line, deg

i_t angle of incidence of horizontal tail with respect to fuselage reference line, deg

H total pressure in tunnel

p static pressure

Subscripts:

o   free stream

1   condition at survey rake (fig. 3)

MODEL AND APPARATUS

The model used in the present investigation was a 1/6-scale model of the MX-1764 airplane. The wing and horizontal-tail surfaces had leading-edge sweep of $55°$, taper ratio of zero, and a small amount of sweepback of the trailing edges ($10°$ for wing and $15°$ for tail). The physical characteristics of the model are presented in figure 2.

Plan views of the duct-inlet configurations investigated and the location of the tubes in the survey rake are shown in figure 3. A fuselage boundary-layer gutter was used for all inlet configurations. Inlet numbers 1 and 3 had the same plan-form characteristics, but the lip of duct 3 had a blunter section than that of the lip of duct number 1.

Provisions were made to pivot the all-moveable horizontal tail at a point 86 percent of the tail root chord and 0.58 inch above the horizontal-tail chord line.

TESTS

The tests were conducted in the Langley 300 MPH 7- by 10-foot tunnel on the single strut support system at a dynamic pressure of 99.8 lb/sq ft, which corresponds to an airspeed of approximately 180 mph. The Reynolds number for these tests, based on a mean aerodynamic chord of the model (22.36 in.), was approximately 3.35×10^6. The angle-of-attack range for these tests was from approximately $-6°$ to the stall.

CORRECTIONS

The angle of attack and drag have been corrected for jet-boundary effects computed on the basis of unswept wings by the method of reference 1. The jet-boundary corrections applied are

$$\Delta\alpha = 0.591C_L$$

and

$$\Delta C_X = -0.0103 C_L{}^2$$

jet-boundary corrections have not been applied to the pitching-moment coefficients because estimations have indicated that these corrections are negligible.

Tare corrections from the single-support strut were not applied to the data. Tare corrections determined on another model of similar size and test setup have shown that the largest effect of the strut is generally on longitudinal-force coefficient and pitching-moment coefficient, which would be increased approximately 0.01 and 0.005, respectively, in the positive direction for the present model.

The data have been corrected for tunnel air-flow misalinement, tunnel blockage, and longitudinal-pressure gradient in the tunnel.

PRESENTATION OF RESULTS

In order to expedite the results of the present investigation, the data are presented with a minimum of analysis. The effects of the jet-engine air-inlet configurations on the longitudinal aerodynamic characteristics in pitch are presented in figure 4. Figure 4(a) presents the longitudinal aerodynamic characteristics of the plain wing configuration with and without the horizontal tail installed. Figures 4(b) to (e) show the longitudinal aerodynamic characteristics of the model with the various inlet configurations (see fig. 3) installed for both the horizontal-tail-on and horizontal-tail-off conditions. It should be noted that the vertical tail was removed for some of these tests. This removal might cause a slight difference in longitudinal force, but it is felt that there would be no significant effect on the lift or pitching characteristics of the model. The effects of horizontal-tail incidence on the longitudinal aerodynamic characteristics of the MX-1764 model without air intake are presented in figure 5.

As shown by a comparison of the variation of pitching-moment coefficient with lift coefficient for the model with various inlet configurations tested (fig. 6), the addition of all inlet configurations generally resulted in a slight reduction in longitudinal stability of the model.

The model with inlet number 4, the extended leading-edge inlet (which had the largest plan-form area ahead of the center of moments), was less stable than with any of the other inlets tested and indicated

an unstable break of the pitching-moment curve at the stall. In general, the maximum lift coefficient was greater for the model with inlets than with the plain wing configuration. (See fig. 4.)
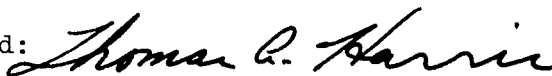
Table I gives the pressure coefficients in the form $\dfrac{H_0 - H_1}{H_0 - p_0}$ for the total-pressure tubes (numbers 1 to 13) and $\dfrac{H_0 - p_1}{H_0 - p_0}$ for the static-pressure tubes (numbers 14 to 17) as shown in figure 3. In conjunction with these data, the free-stream dynamic pressure q_0 and the mass density of air ρ are given so that the mass flow of air through the ducts can be obtained. It should be kept in mind that the increment between the pressure coefficients $\dfrac{H_0 - H_1}{H_0 - p_0}$ and $\dfrac{H_0 - p_1}{H_0 - p_0}$ is a direct indication of the ratio of the dynamic pressure in the duct to the free-stream dynamic pressure.

Langley Aeronautical Laboratory,
    National Advisory Committee for Aeronautics,
        Langley Field, Va., December 22, 1953.

Delwin R. Croom
Aeronautical Research Scientist

Approved:
Thomas A. Harris
Chief of Stability Research Division

pwg

REFERENCE

1. Gillis, Clarence L., Polhamus, Edward C., and Gray, Joseph L., Jr.: Charts for Determining Jet-Boundary Corrections for Complete Models in 7- by 10-Foot Closed Rectangular Wind Tunnels. NACA WR L-123, 1945. (Formerly NACA ARR L5G31.)

TABLE I

PRESSURE COEFFICIENT $\dfrac{H_o - H_1}{H_o - p_o}$ FOR TOTAL-PRESSURE TUBES (NUMBERS 1 TO 13) AND

PRESSURE COEFFICIENT $\dfrac{H_o - p_1}{H_o - p_o}$ FOR STATIC-PRESSURE TUBES (NUMBERS 14 TO 17)

[Tube locations are shown in figure 3]

(a) For inlet 1, ρ = 0.002372

Tube	Values of α, deg										
	-6	-4	0	4	8	12	16	20	22	24	26
1	0.527	0.534	0.549	0.498	0.732	0.606	0.682	0.737	0.769	0.811	0.847
2	.470	.474	.493	.441	.507	.556	.641	.703	.739	.786	.828
3	.431	.420	.448	.418	.466	.518	.613	.688	.725	.777	.820
4	.406	.387	.414	.413	.444	.486	.599	.679	.725	.777	.817
5	.398	.379	.413	.423	.432	.476	.593	.681	.722	.787	.823
6	.217	.202	.250	.279	.299	.379	.477	.622	.699	.764	.804
7	.171	.130	.163	.264	.289	.389	.465	.637	.719	.782	.817
8	.205	.143	.133	.331	.353	.456	.507	.673	.749	.807	.833
9	.373	.327	.316	.461	.479	.556	.596	.733	.790	.839	.861
10	.447	.444	.454	.439	.486	.603	.692	.762	.792	.838	.857
11	.457	.440	.409	.431	.482	.635	.725	.791	.819	.858	.875
12	.520	.494	.423	.439	.527	.673	.765	.824	.851	.883	.896
13	.678	.650	.619	.626	.679	.777	.836	.888	.906	.928	.934
14	.885	.871	.874	.882	.890	.908	.927	.959	.964	.979	.981
15	.918	.906	.907	.915	.921	.933	.948	.978	.979	.994	.987
16	.890	.876	.882	.882	.891	.908	.927	.959	.966	.979	.977
17	.915	.904	.900	.909	.918	.931	.947	.974	.979	.992	.986
q_o	98.47	99.12	99.33	98.90	99.33	98.63	98.42	98.00	98.86	98.37	99.66

TABLE I.- CONTINUED

PRESSURE COEFFICIENT $\dfrac{H_o - H_1}{H_o - p_o}$ FOR TOTAL-PRESSURE TUBES (NUMBERS 1 TO 13) AND

PRESSURE COEFFICIENT $\dfrac{H_o - p_1}{H_o - p_o}$ FOR STATIC-PRESSURE TUBES (NUMBERS 14 TO 17)

[Tube locations are shown in figure 3]

(b) For inlet 2, $\rho = 0.002321$

Tube	Values of α, deg									
	-6	-4	0	4	8	12	16	20	24	26
1	0.520	0.527	0.522	0.527	0.577	0.597	0.647	0.745	0.795	0.827
2	.458	.465	.460	.471	.529	.550	.602	.708	.770	.806
3	.423	.414	.424	.441	.507	.525	.580	.695	.762	.799
4	.401	.394	.410	.432	.495	.517	.570	.685	.758	.795
5	.415	.424	.430	.451	.485	.500	.555	.664	.748	.782
6	.257	.275	.317	.365	.432	.475	.555	.641	.733	.772
7	.204	.225	.262	.328	.394	.492	.569	.624	.735	.772
8	.239	.247	.249	.326	.389	.527	.602	.641	.757	.789
9	.391	.390	.372	.411	.474	.597	.665	.696	.794	.821
10	.515	.492	.454	.432	.439	.444	.497	.619	.735	.779
11	.532	.502	.457	.429	.422	.450	.499	.628	.733	.780
12	.585	.558	.519	.495	.490	.517	.555	.661	.758	.797
13	.715	.700	.669	.656	.657	.679	.705	.779	.669	.863
14	.883	.880	.876	.877	.881	.887	.904	.933	.947	.947
15	.914	.911	.906	.908	.911	.917	.932	.953	.960	.962
16	.888	.884	.877	.878	.882	.889	.906	.936	.943	.947
17	.908	.909	.902	.907	.904	.912	.927	.951	.955	.957
q_o	98.90	97.82	99.12	98.26	99.12	99.12	99.12	98.47	98.26	98.04

TABLE I.- CONTINUED

PRESSURE COEFFICIENT $\dfrac{H_0 - H_1}{H_0 - p_0}$ FOR TOTAL-PRESSURE TUBES (NUMBERS 1 TO 13) AND

PRESSURE COEFFICIENT $\dfrac{H_0 - p_1}{H_0 - p_0}$ FOR STATIC-PRESSURE TUBES (NUMBERS 14 TO 17)

[Tube locations are shown in figure 3]

(c) For inlet 3, $\rho = 0.002320$

Tube	Values of α, deg										
	-6	-4	0	4	8	12	16	20	22	24	26
1	0.530	0.541	0.528	0.494	0.570	0.616	0.682	0.737	0.764	0.801	0.830
2	.482	.477	.478	.438	.517	.571	.640	.709	.732	.776	.809
3	.452	.429	.441	.409	.482	.536	.613	.690	.720	.767	.804
4	.434	.403	.421	.408	.467	.509	.600	.683	.715	.764	.800
5	.419	.393	.428	.424	.440	.479	.576	.672	.713	.765	.804
6	.264	.201	.250	.291	.304	.364	.461	.611	.673	.747	.792
7	.214	.120	.151	.283	.290	.379	.444	.618	.688	.764	.799
8	.239	.141	.113	.361	.349	.439	.479	.653	.723	.792	.822
9	.389	.342	.305	.483	.477	.544	.570	.702	.765	.828	.850
10	.439	.455	.463	.449	.502	.595	.678	.744	.781	.826	.845
11	.455	.455	.433	.449	.515	.630	.717	.771	.804	.848	.865
12	.519	.513	.449	.453	.554	.673	.757	.804	.838	.877	.889
13	.677	.668	.632	.629	.695	.779	.829	.873	.898	.927	.932
14	.879	.891	.882	.882	.887	.906	.918	.946	.962	.981	.977
15	.912	.929	.910	.912	.919	.933	.941	.963	.977	.995	.990
16	.884	.898	.885	.880	.891	.906	.920	.946	.962	.979	.979
17	.909	.922	.905	.907	.914	.928	.925	.963	.977	.995	.990
q_0	99.12	96.32	99.33	99.33	99.12	98.63	98.63	98.63	98.21	98.00	99.02

TABLE I.- CONCLUDED

PRESSURE COEFFICIENT $\dfrac{H_0 - H_1}{H_0 - P_0}$ FOR TOTAL-PRESSURE TUBES (NUMBERS 1 TO 13) AND

PRESSURE COEFFICIENT $\dfrac{H_0 - P_1}{H_0 - P_0}$ FOR STATIC-PRESSURE TUBES (NUMBERS 14 TO 17)

[Tube locations are shown in figure 3]

(d) For inlet 4, $\rho = 0.002365$

| Tube	Values of α, deg										
	-6	-4	0	4	8	12	16	20	22	24	26
1	0.524	0.480	0.475	0.500	0.524	0.549	0.616	0.690	0.731	0.766	0.808
2	.475	.404	.408	.450	.466	.483	.566	.648	.697	.741	.783
3	.450	.370	.366	.416	.425	.433	.533	.623	.680	.724	.774
4	.450	.362	.358	.416	.400	.408	.508	.614	.671	.724	.774
5	.408	.379	.375	.408	.383	.416	.491	.606	.654	.715	.774
6	.291	.194	.216	.316	.266	.325	.400	.539	.594	.665	.724
7	.275	.143	.192	.333	.283	.350	.441	.572	.620	.682	.733
8	.325	.160	.225	.400	.366	.433	.516	.623	.663	.724	.766
9	.458	.337	.358	.516	.483	.533	.608	.690	.723	.766	.816
10	.441	.438	.425	.433	.466	.549	.633	.707	.740	.791	.824
11	.466	.438	.433	.441	.483	.566	.658	.732	.766	.816	.832
12	.533	.505	.500	.500	.533	.624	.699	.766	.800	.833	.857
13	.691	.656	.658	.666	.691	.749	.791	.842	.869	.892	.907
14	.924	.875	.874	.882	.891	.899	.907	.943	.955	.968	.966
15	.957	.901	.907	.916	.924	.924	.932	.959	.972	.985	.982
16	.924	.875	.874	.882	.891	.899	.907	.943	.955	.968	.966
17	.949	.892	.907	.916	.924	.924	.932	.959	.972	.985	.982
q_0	99.05	97.97	99.05	99.05	99.05	99.05	99.05	97.97	95.83	97.97	99.05
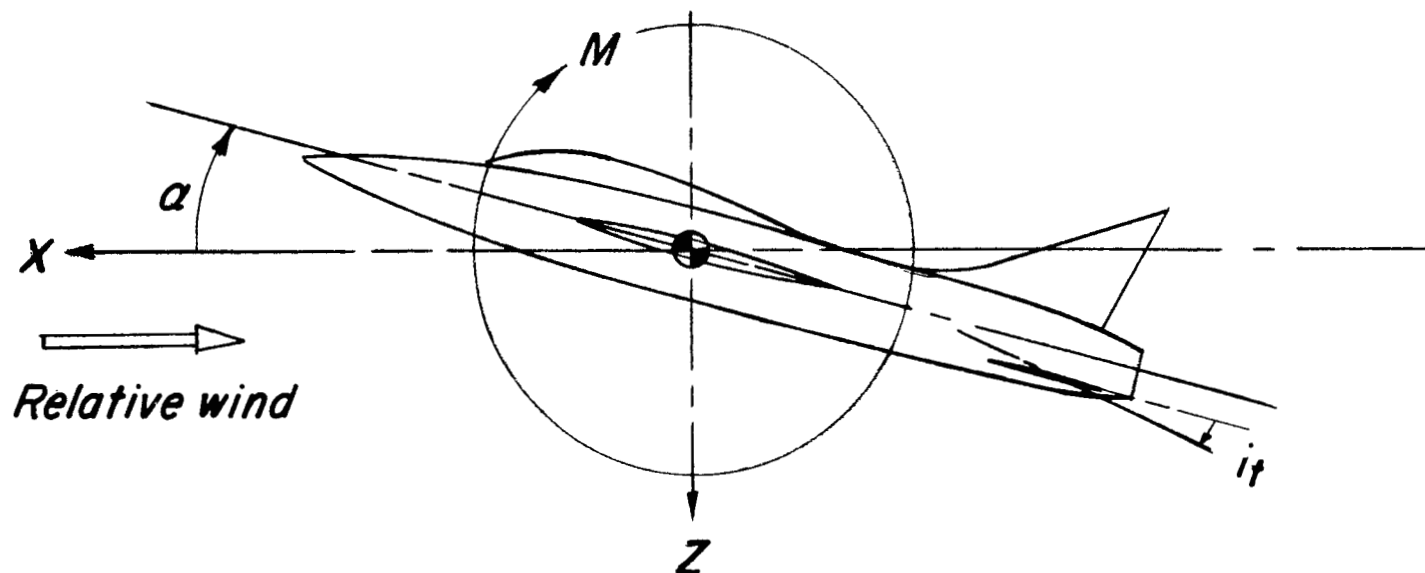
Figure 1.- System of axes and control-surface deflections. Positive
direction of forces, moments, and angles is indicated by arrows.

Physical Characteristics

Wing

Aspect ratio	3.2
Span	53.59 in.
Area	6.25 sq ft
Root chord	33.54 in.
Mean aerodynamic chord	22.36 in.
Airfoil section (parallel to air stream)	65A004.5
Sweepback	
Leading edge	55°
Trailing edge	10°
Incidence	0°

Horizontal tail

Aspect ratio	3.4
Area (total)	1.41 sq ft
Airfoil section	65A004.5

Vertical tail

Area (exposed)	.89 sq ft
Airfoil section	65A004.5

Figure 2.- Three-view drawing of the 1/6-scale model of the MX-1764 air-
plane. All dimensions are in inches.

CONFIDENTIAL

Section A-A
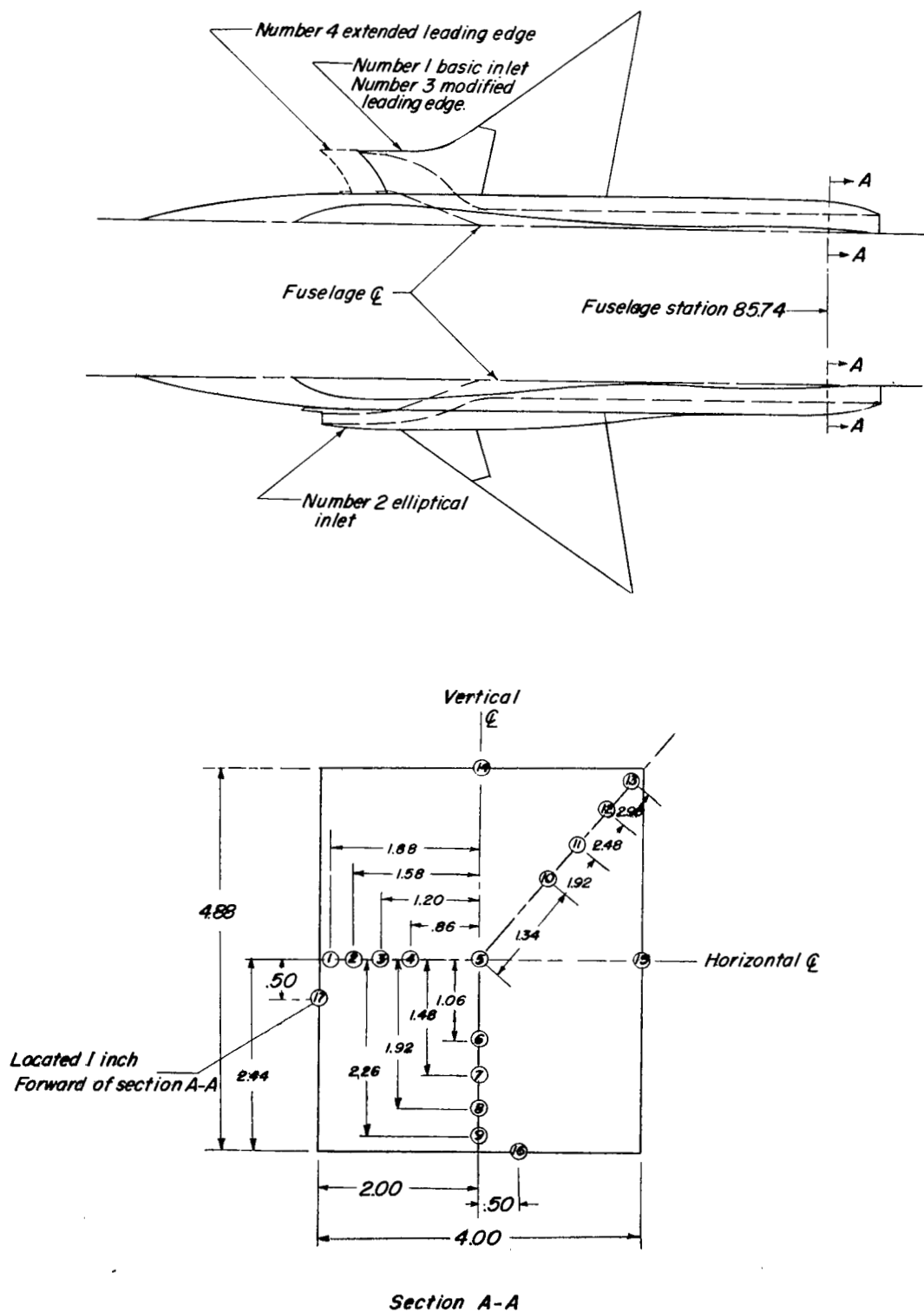
Figure 3.- Plan view of inlets tested and internal pressure-tube locations.

Inlet number 1

Boundary-layer gutter

Inlet number 3

Fuselage ₵

Inlet number 4
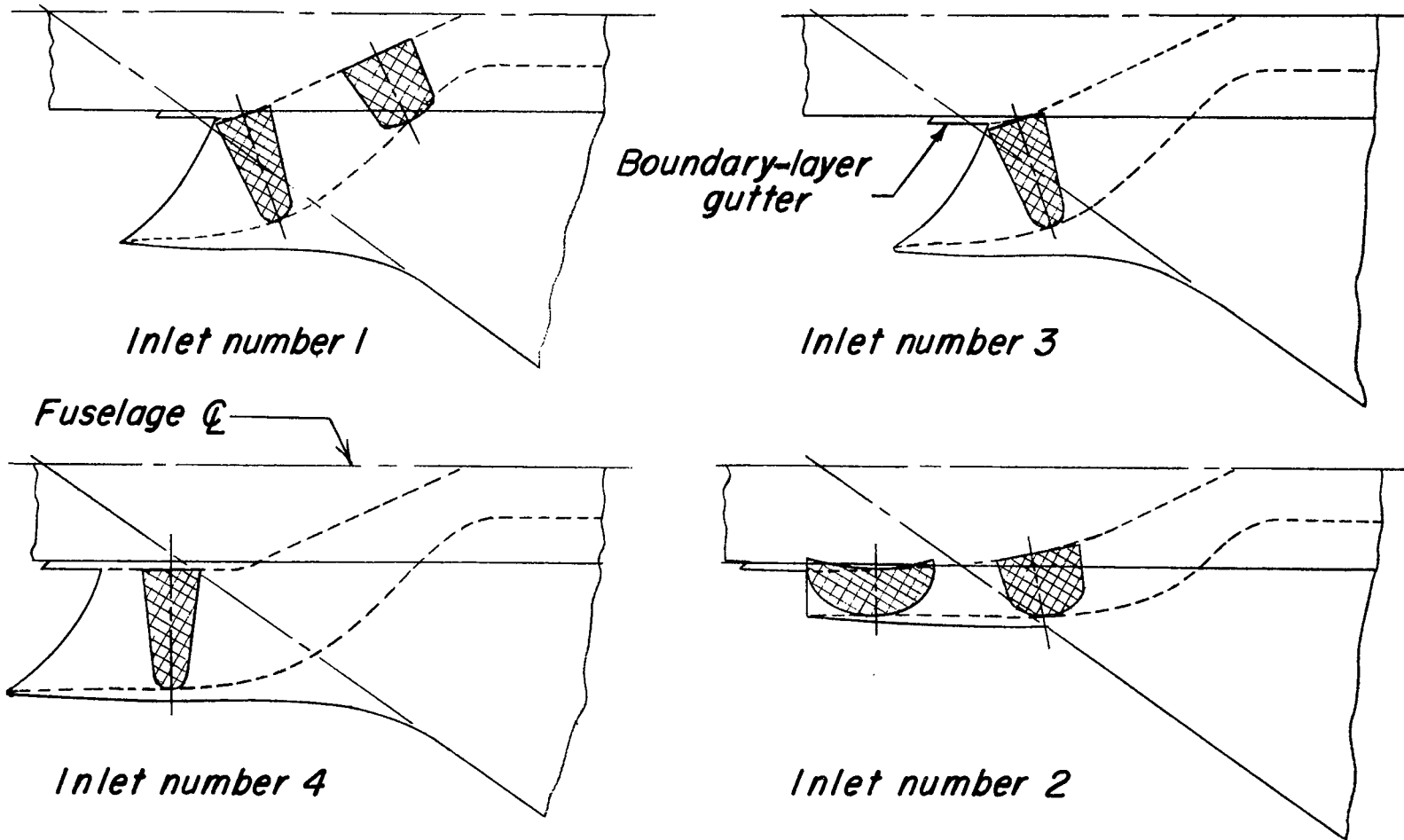
Inlet number 2

Plan form of inlets

Figure 3.- Concluded.
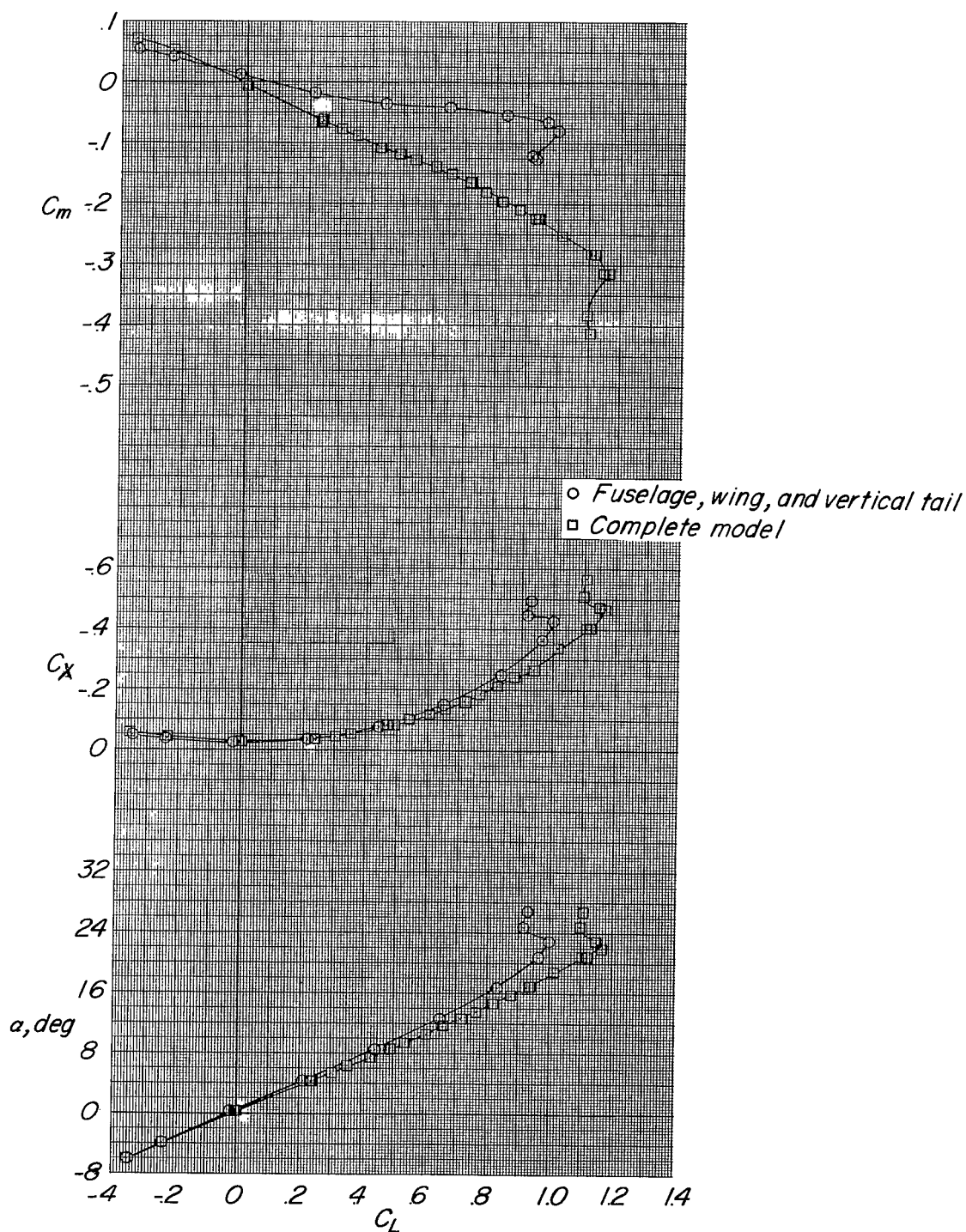
(a) Plain wing configuration.

Figure 4.- Aerodynamic characteristics in pitch of the 1/6-scale model of the MX-1764 airplane. $i_t = 0°$.
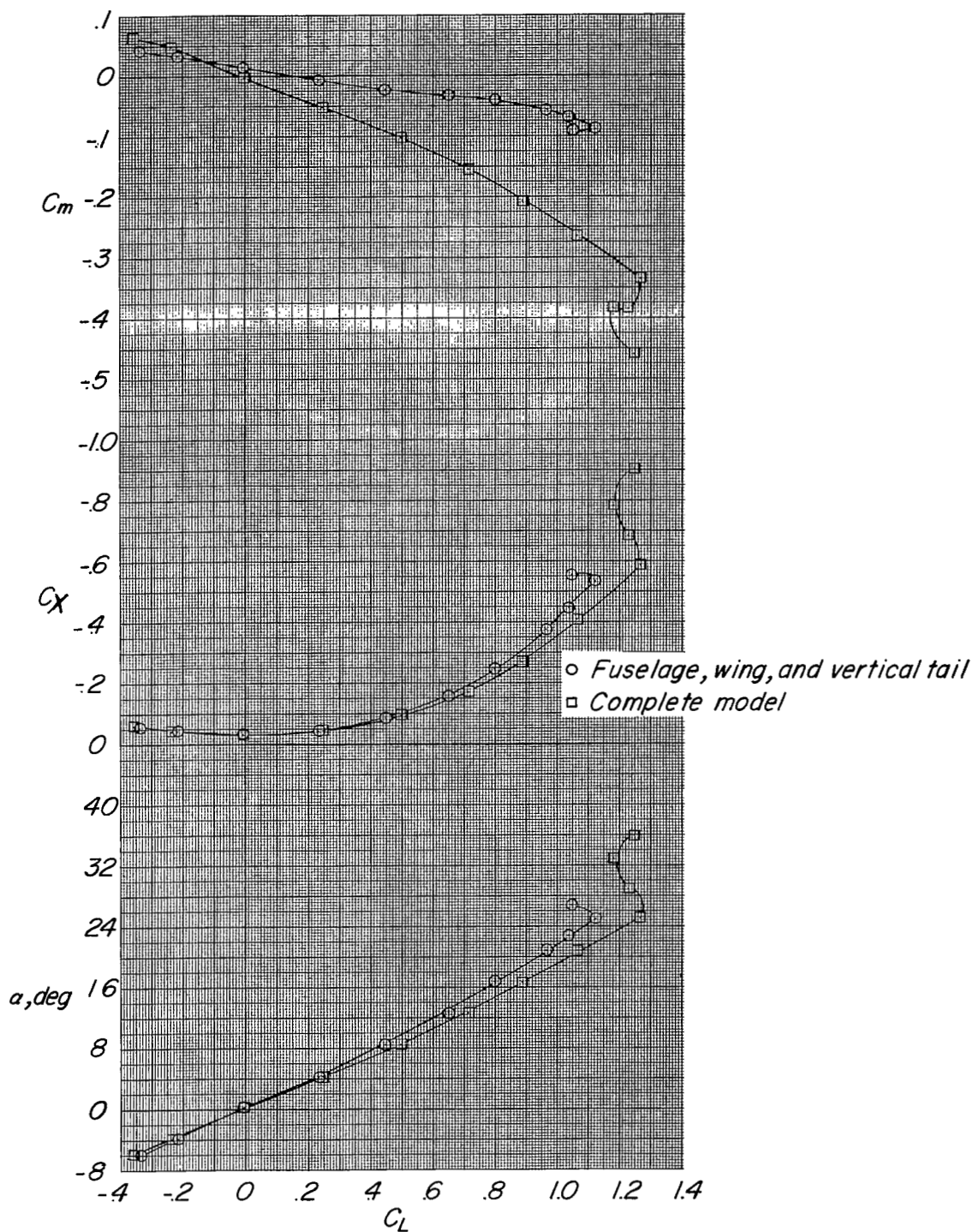
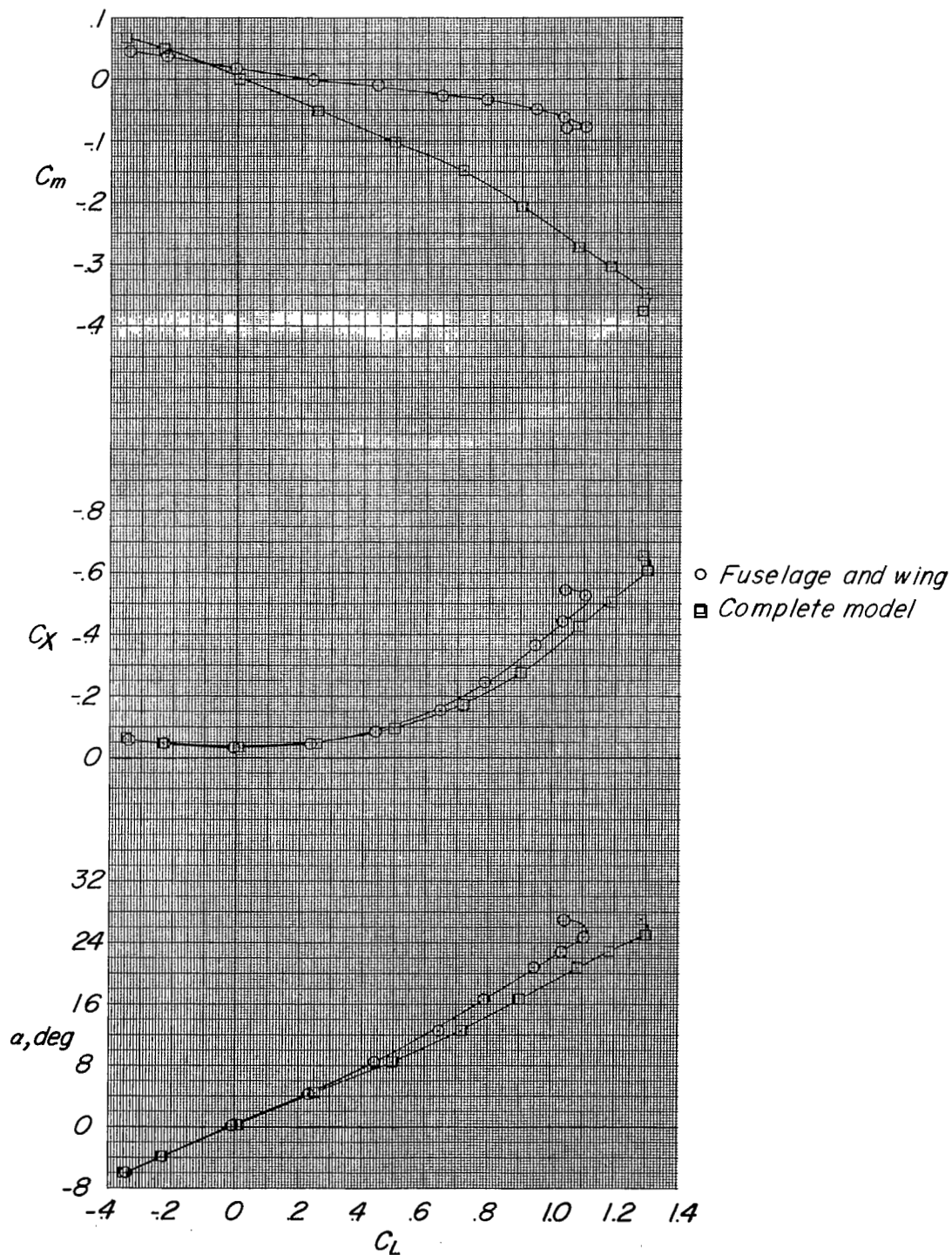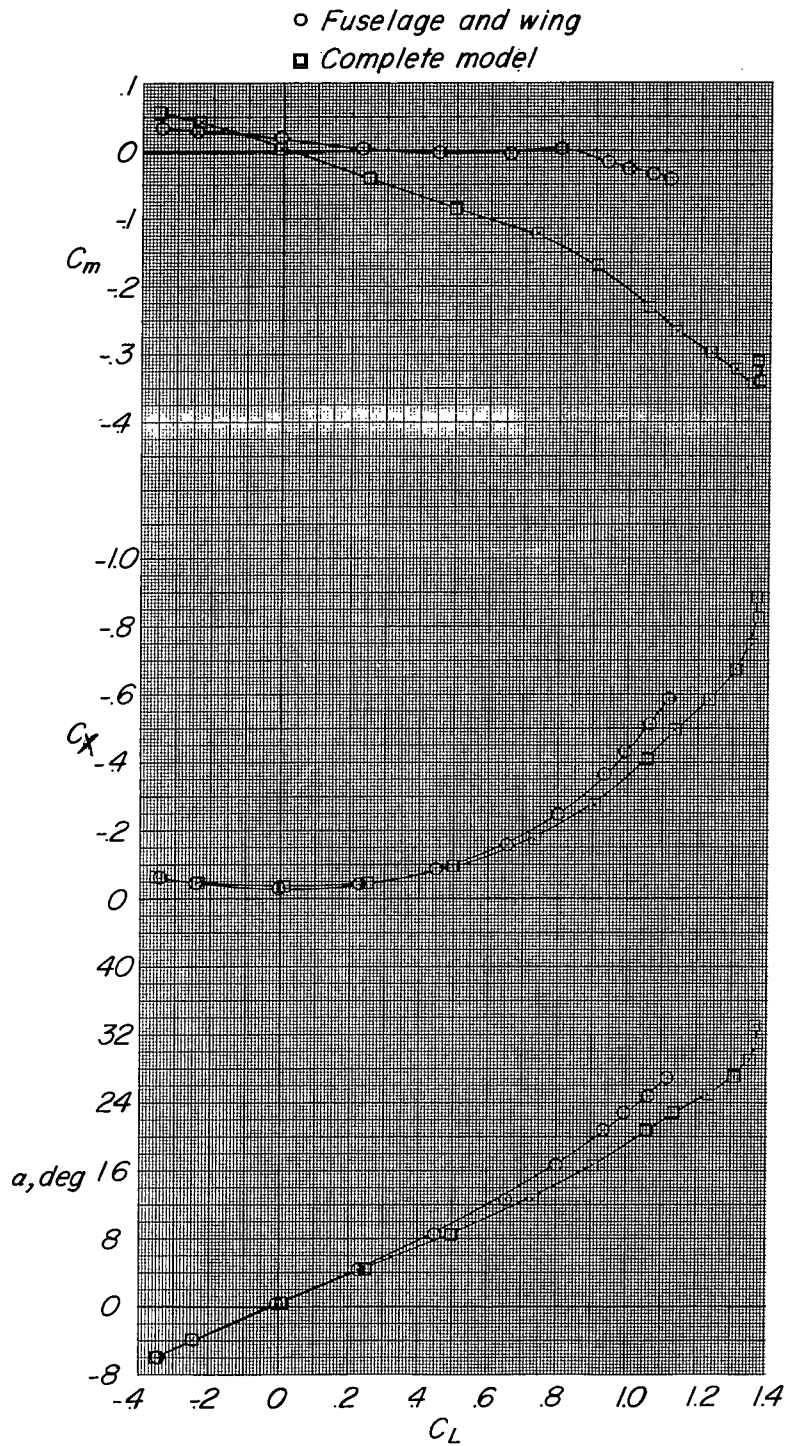(b) Inlet number 1.

Figure 4.- Continued.

○ *Fuselage and wing*
□ *Complete model*

(c) Inlet number 3.

Figure 4.- Continued.

o Fuselage and wing
□ Complete model

(d) Inlet number 4.

Figure 4.- Continued.

○ Fuselage and wing
□ Complete model
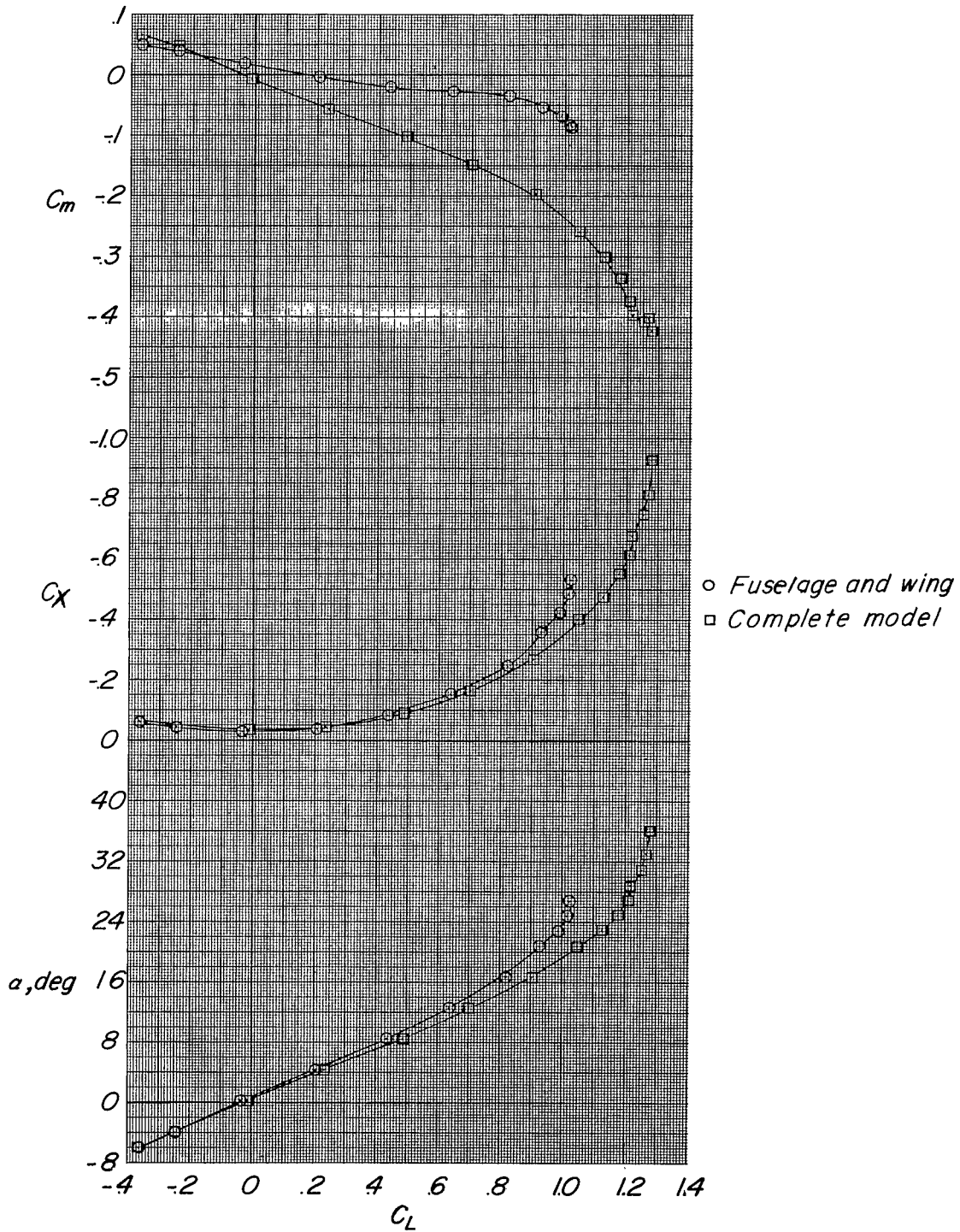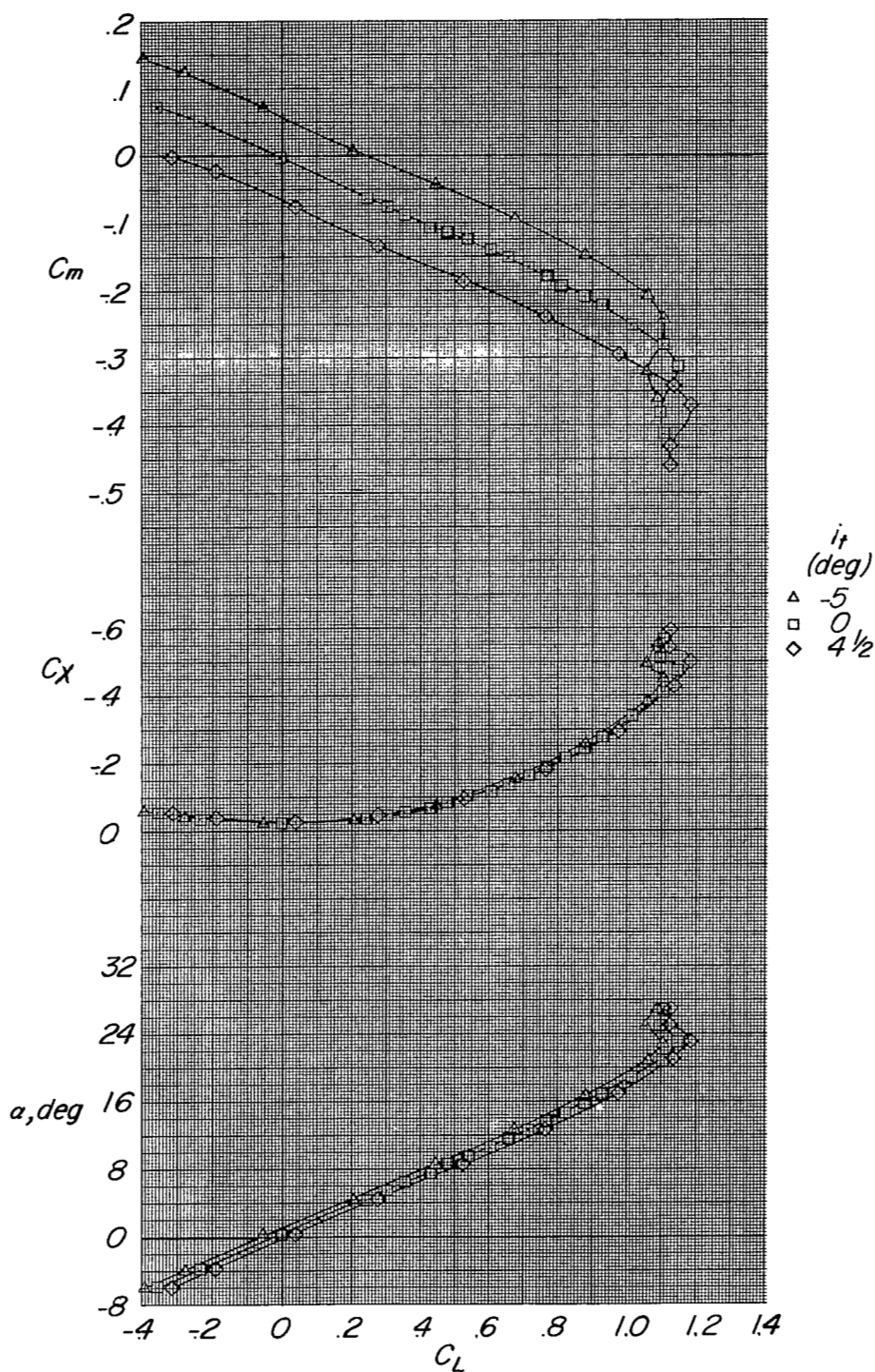
(e) Inlet number 2.

Figure 4.- Concluded.

Figure 5.- Effect of tail incidence on aerodynamic characteristics in pitch of the 1/6-scale model of the MX-1764 airplane (plain wing configuration).
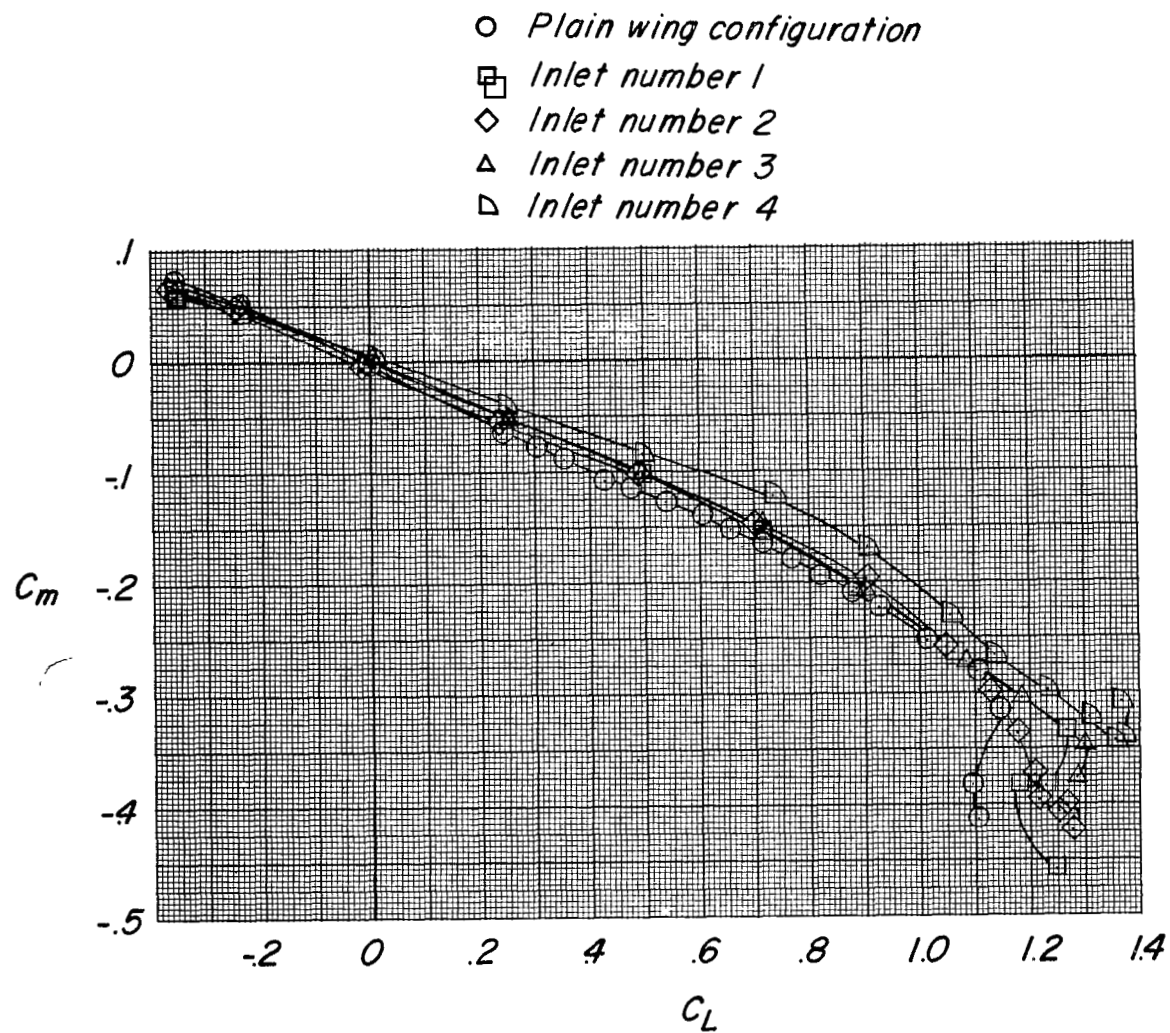
Figure 6.- Variation of pitching-moment coefficient with lift coefficient for all complete model configurations tested. $i_t = 0°$.